Article

Otolith morphometric analysis of North Bornean Ariidae (Siluriformes): new insights and taxonomic implications

ADIBAH JOHARI[1*], LÁSZLÓ KOCSIS[2], AMAJIDA ROSLIM[1] & ILMAN HAZIQ[1]

[1]*Geosciences programme, Faculty of Science, Universiti Brunei Darussalam, Bandar Seri Begawan, Jalan Tungku Link, Gadong BE1410, Brunei Darussalam*

✉ *amajida.roslim@ubd.edu.bn;* ⓘ *https://orcid.org/0000-0003-4923-752X*

✉ *ilmanhaziqhjabdullah@gmail.com;* ⓘ *https://orcid.org/0009-0003-1471-8531*

[2]*Institute of Earth Surface Dynamics, University of Lausanne, Lausanne, Switzerland*

✉ *laszlo.kocsis@unil.ch;* ⓘ *https://orcid.org/0000-0003-4613-1850*

Corresponding author: ✉ *adibahsyahirah97@gmail.com;* ⓘ *https://orcid.org/0009-0007-6991-7641*

Abstract

This study examines the morphometric variation of lapilli otoliths in selected modern sea catfish species (Ariidae, Siluriformes) from northern Borneo. Given the pronounced similarity in otolith shape and anatomical features among these taxa, traditional taxonomic discrimination is often challenging, particularly at the species or genus level. To assess the taxonomic utility of otolith morphology, 216 otoliths from 12 species were analyzed using high-resolution imaging, a suite of shape indices (*e.g.*, form factor, roundness), and precise measurements of defined ventral features (*e.g.*, linea basalis). Seventeen morphometric parameters were subjected to various statistical analyses, including Principal Component Analysis (PCA), which delineated two major groups based on otolith shape. The rounded group comprised species from the genera *Hexanematichthys*, *Netuma* (two species), and *Plicofollis* (two species), while the elongated group included species from *Arius* (three species), *Batrachocephalus*, *Cryptarius*, *Kyataphisa*, and *Osteogeneiosus*. Subsequent statistical comparisons of selected morphological parameters revealed significant differences among some taxa. *Hexanematichthys sagor* exhibited a distinctly circular otolith morphology, characterized by a low aspect ratio (AR) and a uniquely oriented distal edge (AP6). Within the elongated group, although the parameters varied less, their combined assessment showed promise in differentiating certain taxa, such as *Cryptarius* and *Osteogeneiosus*, particularly through measurements of the otolith central area (R1), incisura linea basalis width (AP1), and otolith thickness ratio (R2). These findings demonstrate that even subtle morphological differences in otoliths can be quantitatively resolved to enhance taxonomic differentiation among ariid catfishes.

Key words: Shape indices, Sulcus morphology, Taxonomy, Lapilli otolith

Introduction

The family Ariidae, also known as sea catfishes, belongs to the order Siluriformes and comprises about 40 genera and 160 species, of which 51 occur in Southeast Asia (Ferraris, 2007; Betancur-R, 2009; Froese & Pauly, 2024; Marceniuk *et al*. 2024, see also Supplementary data 1). Its members are typically distributed across tropical and subtropical regions (Marceniuk & Menezes, 2007; Simier *et al*. 2021), making Southeast Asia an important region for Ariidae abundance and diversity. They possess a unique skeletal structure in which small skull bones known as the Weberian apparatus help to stabilize pressure changes, thereby enabling these fishes to adapt to a variety of environments (Dantas *et al*. 2010). Although ariids are predominantly marine, some species frequently inhabit brackish waters such as coastal lagoons or estuaries, and a few even venture into freshwater environments in search of adequate food (Pusey *et al*. 2020). Typically, they are found on muddy or sandy bottoms and exhibit a demersal lifestyle (Burgess, 1989; Marceniuk & Menezes, 2007).

Ariids exhibit considerable size variation among species, with maximum lengths ranging from approximately 20 to 180 cm. Similar to other catfish families, most ariids possess barbels arranged in three pairs—the maxillary, mandibular, and mental—which function as sensory organs to locate and identify food (Acero, 2002). Their body

---

colouration varies from dark brown to charcoal as well as dark and pale blue-brown, often accompanied by a lustrous sheen in blue, green, violet, or copper tones. Two key head features distinguish ariids: the uniquely patterned, granulated bony skull plates that form the head shield, and the palatal tooth patches located on the roof of the mouth (Fig. 1). Ariids lack scales and generally exhibit deeply forked caudal fins (Acero, 2002).
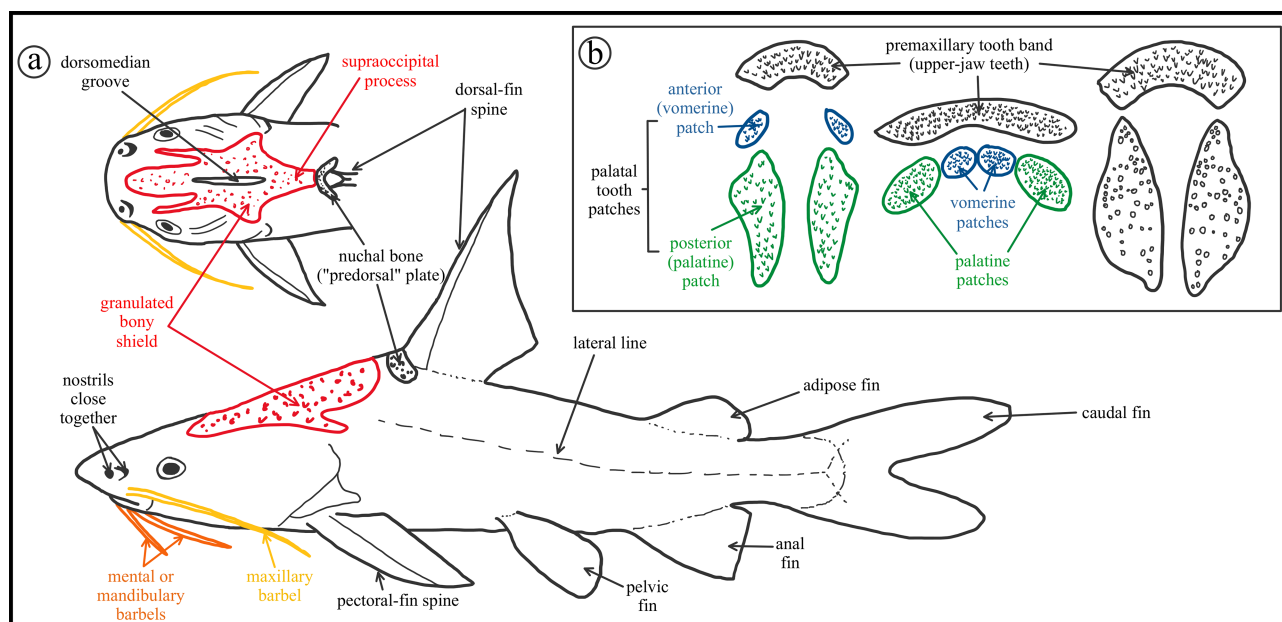

FIGURE 1. Illustration of a typical Ariidae. **a:** ariid body terminologies, **b:** examples of ariid tooth patches on the palate (roof of the mouth) and upper jaw. Based on Kailola (1999).

Although the external features of ariid fishes are essential for taxonomic identification, classifying some species remains challenging because many exhibit nearly indistinguishable external appearances (*e.g.*, Abdurahman *et al*. 2016). Moreover, morphological variations, often due to sexual dimorphism and ontogenetic changes, further complicate species differentiation (Marceniuk *et al.* 2012, 2017). Although regional taxonomic guides exist to aid in the identification of sea catfishes (*e.g.*, Kailola & Bussing, 1995; Kailola, 1999), analyzing otolith morphology can provide additional distinguishing features for each ariid species and enhance our overall understanding of Ariidae biology.

In this study, we explore variation of otolith (ear stone) morphology of selected Southeast Asian ariid taxa and test whether the result could provide further taxonomic importance. Otoliths are calcareous structures within the inner ear, the vestibular labyrinth of fishes, and they are surrounded by clear endolymph fluid (Bond, 1996). Their functions are mainly associated with sense of balance, orientation, and sound reception (Nolf, 1985, 2013). Their shape is variable and useful for understanding fish systematics, ontogeny, and evolution (Popper *et al.* 2005). Consequently, otolith morphometry is a widely known technique to measure fish biodiversity and it has been applied to many taxonomic and phylogenetic studies (Tuset *et al.* 2016).

Otoliths are typically found in three pairs and are classified into three types: saccular (sagitta), lagenar (asteriscus), and utricular (lapillus). Both the sagittae and lapilli are primarily composed of aragonite, while asterisci are mainly made up of vaterite. In most teleosts, the sagittae are the largest; however, in ariids the lapilli are enlarged and are dorsoventrally flattened, with their mesial side slightly inclined dorsally (Aguilera *et al.* 2020). The first comprehensive studies on ariid otoliths were conducted on species from the East China Sea (Ohe, 2000) and Malaysia (Ohe, 2006). In these papers, Ohe described the key features of lapillus otoliths and introduced several terminologies adopted in subsequent research. He investigated twelve Ariidae species and categorized their otoliths into three morpho-groups: macula shaped (otoliths appear oval), clam shaped (otoliths appear circular), and an intermediate group in which the otoliths display shapes that fall between oval and circular (Ohe, 2006).

Other detailed studies on ariid otoliths come from the South American regions in which comparative skull morphology, several micro-CT scans, and radiographs of the skulls are provided, where the position and the shape of the otoliths can be observed (Aguilera *et al.* 2013, 2020). Otolith terminology has also been extended and applied to

Brazilian ariids (Santificetur *et al.* 2017). Later studies used other sophisticated morphometric techniques and related statistical analyses to attempt visualizing taxonomical differences. Arroyo-Zúñiga *et al.* (2022), used geometric morphometrics on 199 otoliths coming from eight north-eastern Pacific ariid species, and found that the lapillus shape is very useful for distinguishing the examined taxa. Farooq & Panhwar (2023) studied nine sympatric sea catfishes in Pakistan in the western Indian Ocean Region and showed that adding otolith shape parameters to fish taxonomy can help further differentiation among some ariids. They included morphometric parameters from otoliths of 832 specimens in their database and carried out discriminant function analyses. Maciel *et al.* (2019) noted that there is a possibility of otolith morphological variation in the same ariid species especially during mating season. For example, *Genidens genidens*, a South American ariid species, showed significant differences in head and mouth measurements, and this is believed to be mainly related to the oropharyngeal incubation of offspring carried out by males. Such changes in external appearance could affect the otolith shape as they are trying to accommodate the physical changes the fish has made to its body. Hence, morphometric studies on the ariid otoliths can possibly aid in detecting such variation.

Studies on the morphology and morphometry of Southeast Asian ariids, especially in north Borneo are scarce. Therefore, this study investigates the most commonly encountered north Bornean ariids and their otoliths to mitigate taxonomic complexity. Specifically, the research aims to: (1) propose a clarified terminology for ariid otoliths by incorporating novel features; (2) provide detailed descriptions of the otoliths of the examined taxa, while highlighting potential morphological differences; and (3) present quantitative morphometric data alongside additional otolith-related characters to assess their taxonomic relevance.

Materials and Methods

Studied Materials

The studied fish specimens come from ten localities in northern Borneo, mainly from Brunei Darussalam and Sarawak in Malaysia. Most of the specimens were obtained from fish markets where vendors sell their fish caught mainly in the South China Sea, but the Brunei Bay and Brunei River are also often fished. Additional specimens were collected on the beach as carcases or were caught with fishing lines. Our database includes a total number of 216 Ariidae that belong to twelve species. Their origin is shown in Fig. 2 and listed in Table 1.

TABLE 1. List of the investigated species with their origin and numbers.

Taxa	Label on map	Locality	No. of specimens	Total specimens	Fish total length range (cm)
Arius maculatus	3	Mangrove Paradise Resort	1		
	7	Gadong Wet Market	2	12	17.1–26.1
	8	Jerudong Wet Market	8		
	9	Pondok Pagong-pagong	1		
Arius oetik	8	Jerudong Wet Market	7	7	17.6–22
Arius venosus	8	Jerudong Wet Market	28	28	16–22.4
Batrachocephalus mino	8	Jerudong Wet Market	1	1	21.7
Cryptarius truncatus	7	Gadong Wet Market	5	22	22–42.5
	8	Jerudong Wet Market	17		
Hexanematichthys sagor	3	Mangrove Paradise Resort	1		
	5	Penanjong Beach–P2 block	4	14	21–46
	8	Jerudong Wet Market	7		
	10	Tanjung Batu Beach	1		
Kyataphisa nenga	1	Kg. Sebako–Pulau Bruit	1		
	2	Mukah Fish Market	2	6	20.5–38.3
	8	Jerudong Wet Market	3		

TABLE 1. (Continued)

| Taxa	Label on map	Locality	No. of specimens	Total specimens	Fish total length range (cm)
Netuma bilineata	7	Gadong Wet Market	9	24	22.5–59
	8	Jerudong Wet Market	15		
Netuma thalassina	4	Serasa Market	1	16	34–91
	7	Gadong Wet Market	12		
	8	Jerudong Wet Market	3		
Osteogeneiosus militaris	2	Mukah Fish Market	1	14	18–25.1
	7	Gadong Wet Market	7		
	8	Jerudong Wet Market	6		
Plicofollis argyropleuron	7	Gadong Wet Market	2	39	22.3–55
	8	Jerudong Wet Market	37		
Plicofollis nella	4	Serasa Market	1	33	17.5–78
	6	Jerudong Pantai Caffe Beach	1		
	7	Gadong Wet Market	16		
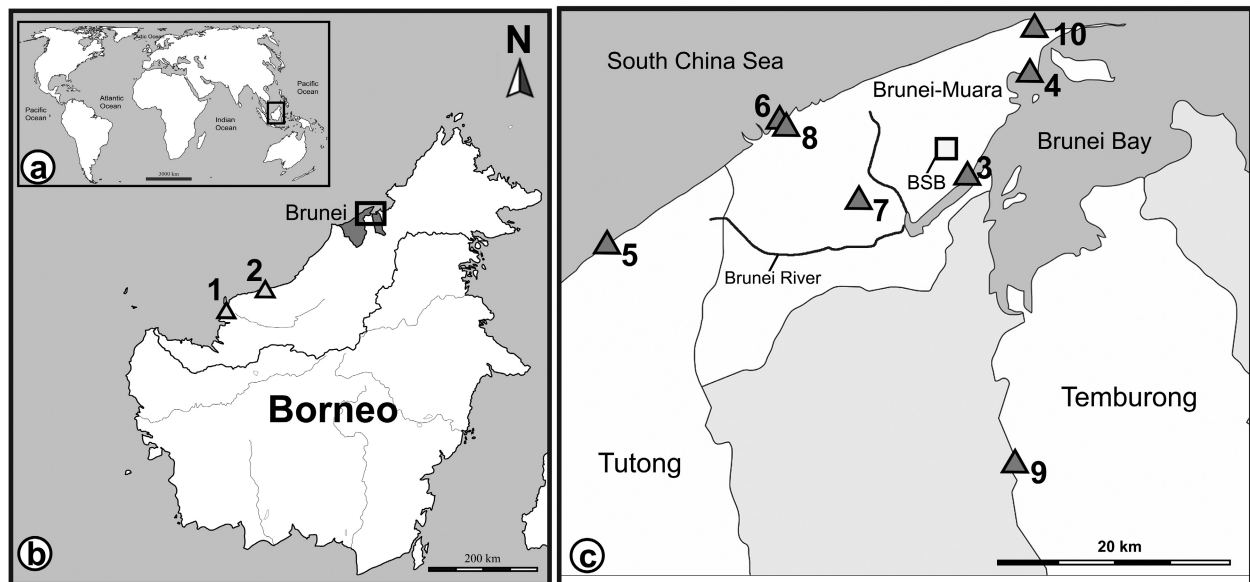
FIGURE 2. Localities where the fish samples were obtained. **(a)** World map, **(b)** Map of Borneo, **(c)** Close-up map of northeastern part of Brunei Darussalam. **1**: Kg. Sebako—Pulau Bruit; **2**: Mukah Fish Market; **3**: Mangrove Paradise Resort; **4**: Serasa Market; **5**: Penanjong Beach—P2 block; **6**: Jerudong Pantai Caffe Beach; **7**: Gadong Wet Market; **8**: Jerudong Wet Market; **9**: Pondok Pagong-pagong; **10**: Tanjung Batu Beach; **Triangles**: locations where Ariidae fishes were bought/collected; **BSB**: Bandar Seri Begawan.

Laboratory work on fish specimens

Prior to otolith extraction, each fish was photographed from dorsal, ventral, and lateral perspectives, and measurements, including total length, standard length, and head length (in cm), were recorded. The head and the lower jaw of the fish specimen were cut off to examine the arrangement of the tooth patches and for easy access to the exoccipital of the ariid cranium (Acero & Betancur-R, 2007), where holes were made for otolith extraction. Following extraction, the lapillus otoliths were cleaned, dried, and stored in pairs in individual zip-lock bags, each labelled with the collection number, date, and location of retrieval.

Brief descriptions on head morphology and tooth patch arrangements of collected ariid species are provided below (see also **Supplementary data 2** and **3**). In addition, the neurocranium of selected specimens for each species are displayed in **Supplementary data 4**. The size range of the fishes relates to total length (TL) and the number of specimens expressed as "n".

Arius maculatus (TL range: 17.1–26.1 cm, n=12)
Head shield ornamentation is striate, rugose, and finely granular. It has two oval-shaped tooth patches that are antero-posteriorly elongated and posteriorly narrow.

Arius oetik (TL range: 17.9–22 cm, n=7)
Head shield is generally smooth anteriorly but is finely granulated towards the supraoccipital. A row of larger dots along the posterior end of the cranial fontanel is always present. It has two triangular tooth patches that are situated anteriorly.

Arius venosus (TL range: 16–22.4 cm, n=28)
It is similar to *A. oetik*, but the head shield possesses larger dots and more granulated ornamentations. The supraoccipital process is less elongated and wider at the base. It has two triangular tooth patches, which are stretched antero-posteriorly.

Batrachocephalus mino (TL size: 21.7 cm, n=1)
It has only one pair of barbel, as it lacks both the maxillary and mental pairs. It has a blunt snout and granulated head shield. Tooth patches are absent, but it has wide band of conical, blunt teeth in both jaws.

Cryptarius truncatus (TL range: 22–42.5 cm, n=22)
Head shield appears smooth anteriorly but becomes rugose to granular posteriorly. It has two small, anteriorly situated, oval-shaped tooth patches that are antero-posteriorly narrowed.

Hexanematichthys sagor (TL range: 21–46 cm, n=14)
The head is broad; with wide head shield that bears striae rugose ornamentation. The supraoccipital process is wide and fan shaped. Nuchal bone is very broad and has a "butterfly" shape. It has four, anteriorly situated, oval-shaped tooth patches that are antero-posteriorly narrowed. The two inner patches are smaller than the two outer ones.

Kyataphisa nenga (formerly known as *Nemapteryx nenga* see Marceniuk *et al*. 2024)
(TL range: 20.5–38.3 cm, n=6)
The head shield is granulated. It bears two roughly triangular tooth patches that are situated anteriorly.

Netuma bilineata (TL range: 22.5–59 cm, n=24)
It has rounded snout. The head shield bears rugose or granular ornamentation, that becomes coarser towards the supraoccipital process. It has six tooth patches, (three on each side of the palate) where two in the middle (vomerine patches) are circular, the other four ovals. The anterior oval-shaped patches (palatine patches) are narrowed antero-posteriorly but can also appear circular in some specimens. The posterior oval-shaped patches are elongated antero-posteriorly.

Netuma thalassina (TL range: 34–91 cm, n=16)
It has a characteristic pointed snout. The head shield is finely granular. It bears six tooth patches (three on each side of palate). Their arrangement and appearance are similar to *N. bilineata*'s.

Osteogeneiosus militaris (TL range: 18–25.1 cm, n=14)
Only maxillary barbels are present, which are long and stiff. The head shield is covered with smooth skin. It has two large longitudinal elliptical patches that anteriorly angled slightly inwards.

Plicofollis argyropleuron (TL range: 22.3–55 cm, n=39)
Head shield has rather granular ornamentation. It has two oval-shaped tooth patches on each side of the palate. They are antero-posteriorly elongated.

Plicofollis nella (TL range: 17.5–78 cm, n=33)
The species has prominent lateral ethmoid (protrusions above eyes). The head shield is rugose. It has four tooth patches, two on each side. The anterior patches are circular, while the posterior patches are oval-shaped, and strongly elongated antero-posteriorly.

Otolith morphological description

Each otolith pair shares the same morphological characteristics; hence, this study only uses the left lapillus to illustrate their morphology. The characteristic features and related nomenclatures follow Ohe (2006), Aguilera *et al*. (2013), and Santificetur *et al*. (2017). The used terminologies are displayed in Fig. 3. Note that some terms used by Ohe (2006) such as antero-sulcus correspond to sulculus lapilli (Sl), while Ohe's cauda and ostium are referred here as mesial shallow depression (Msd). Meanwhile, the term mesial inward curve was used by Aguilera *et al*. (2013), here referred to as incisura linea basalis (ILb) following Santificetur *et al*. (2017).

Otolith morphometrical documentation

The otoliths were photographed in three different views (ventral, dorsal, and mesial) by using a digital microscope (VHX-7000, KEYENCE, University of Lausanne, Switzerland). Most of the morphometric measurements are taken on the ventral surface where three distinct areas are recognized and separated by the linea basalis (Lb): distal area (DA), mesial shallow depression area (MA), and sulculus lapilli area (SA). To determine the shape differences between the ariid otoliths, basic measurements including otolith length (OL), otolith width (OW), otolith thickness (OT), otolith perimeter (OP), and otolith area (OA) were measured by using the VHXAnalyzer Software. Additional measurements such as otolith mass (OM) were recorded using weighing scale, while otolith volume (OV) was measured using water displacement method. Otolith density (OD) was then calculated using the resulting OM and OV values.

Shape indices were introduced to provide numerical values to describe otolith appearance (Souza *et al*. 2020; Ponton, 2006). A total of six shape indices were used in this study, and their related formulas are as follows (Fig. 4A): (1) aspect ratio AR = OL/OW, (2) circularity CI = OP^2/OA, (3) ellipticity EL = (OL–OW)/(OL + OW), (4) form factor FF = $4\pi \times$ OA/OP^2, (5) rectangularity RE = OA/(OL $\times$ OW), and (6) roundness RO = $4OA/ \pi \times OP^2$. It is important to note that while Souza *et al*. (2020) used the term "format factor", Ponton (2006) uses the term "form factor" instead even though both terms are described similarly and share the same formula. To avoid confusion, our study uses the term "form factor" as "format factor" is not a standard term used in a morphological context.

AR expresses the length of the otolith such as higher number indicate more elongated otolith. EL measures the relationship between changes in axes and the oval shape of the otolith. A higher EL value implies that the specimen is more oval in shape, or it is stretched more in one particular direction. FF assesses the uniformity of the otolith's outline, where the smaller the FF value, the lacier the outline of the otolith. RE expresses the closeness of the otolith shape to a rectangle; the closer the index value is to 1, the more rectangular the specimen is. Both CI and RO indicate the degree of similarity of otolith to a circle, however, CI measures how closely the otolith resembles a perfect circle, while RO measures how the shape of an otolith "come close to" that of a perfect circle. Larger values for both CI and RO indicate a more circular otolith shapes, decreasing as the otolith shape deviates from a circle.

Three main ratios were taken: (1) Otolith central area ratio, (2) otolith thickness ratio, and (3), mesial-distal width ratio (Fig. 4B). In addition, eight parameters were also defined based on the ventral features of the otoliths (Fig. 4C), which include: (1) Incisura linea basalis width, (2) mesial notch width, (3) linea basalis starting point, (4) central offset, (5) mesial edge, (6) distal edge, (7) linea basalis length and (8) antero-mesial projection. To take these extra orientation measurements, the otoliths were oriented relative to a horizontal line called the reference line. This is to depict the original position in the otic capsule of the fish skull. Orientation of specimens was measured between the antero-mesial projection (Amp) and the postero-mesial inclination of the mesial margin of the lapillus including
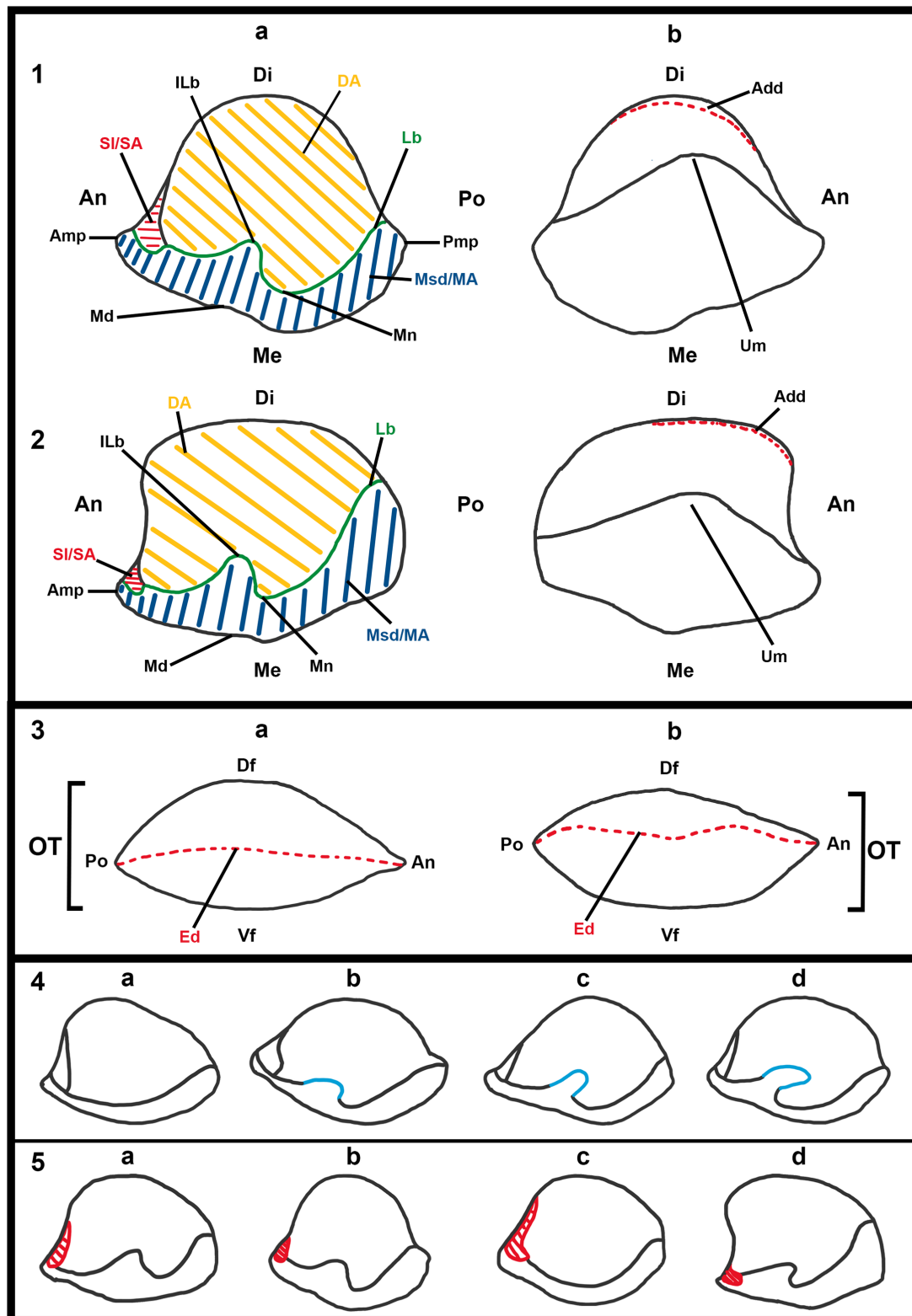
FIGURE 3. Ariidae lapilli otolith morphology. **1a & 1b**: rounded; **2a & 2b**: elongated, **1a & 2a**: ventral view, **1b & 2b**: dorsal view, **3**: mesial view; **1a–b&3a**: *Netuma thalassina*; **2a–b&3b**: *Arius maculatus*; **4**: Variations of incisura linea basalis (ILb) — 4a: absent; 4b: shallow; 4c: deep; 4d: deep bent; **5**: Variations of sulculus lapilli (SI) — 5a: tubular straight; 5b: compact straight; 5c: tubular curved; 5d: compact curved. Abbreviations: **Add**: antero-distal ditch; **Amp**: antero-mesial projection; **An**: anterior; **DA**: distal area; **Di**: distal; **Ed**: edge; **ILb**: incisura linea basalis; **Lb**: linea basalis; **MA**: mesial shallow depression area; **Md**: mesial dent; **Me**: mesial; **Mn**: mesial notch; **Msd**: mesial shallow depression; **OT**: otolith thickness; **Po**: posterior; **Pmp**: postero-mesial projection; **SA**: sulculus lapilli area; **Sl**: sulculus lapilli.
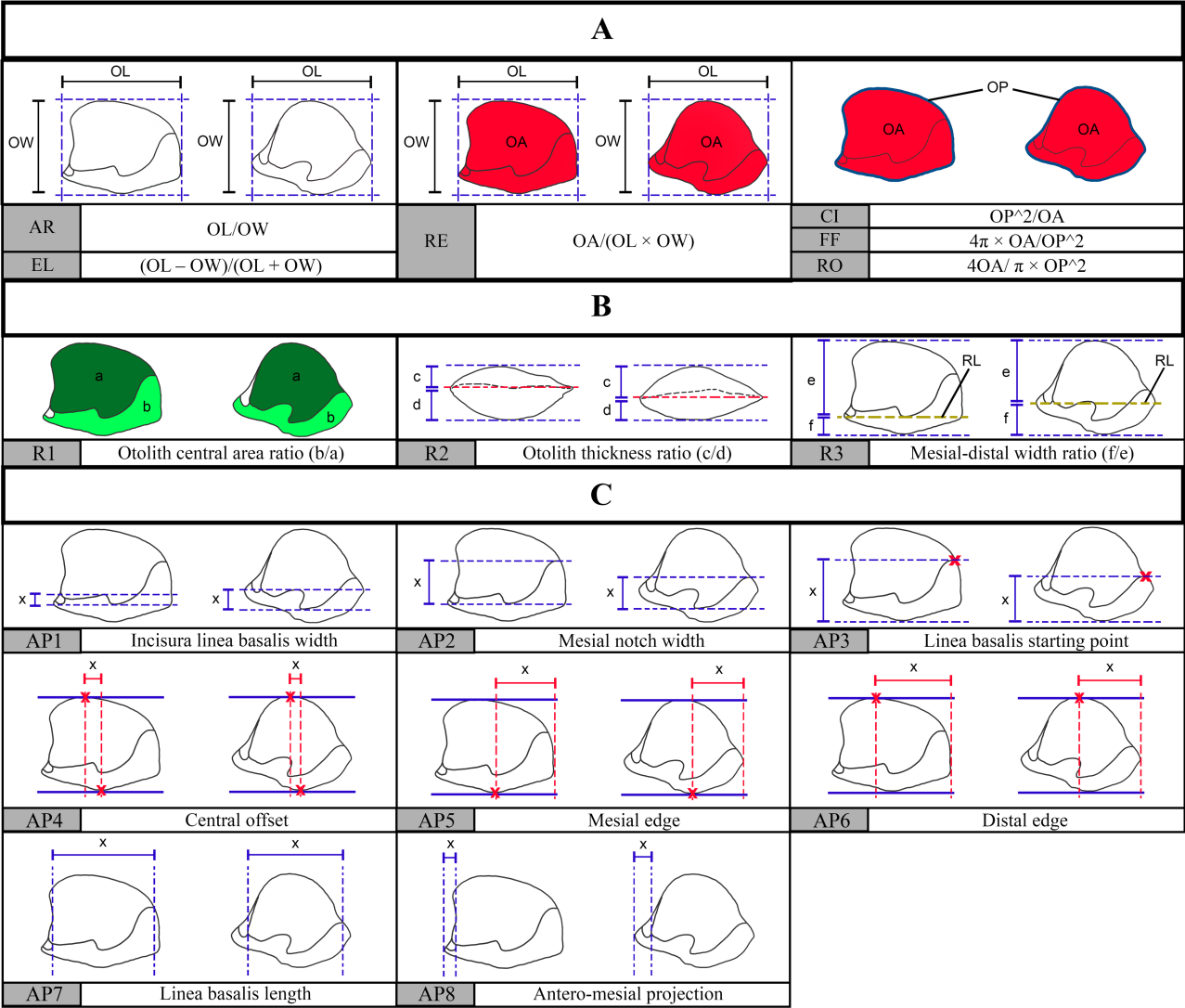
FIGURE 4. Sketches for each otolith parameter. **A**: shape indices, **B**: ratios, **C**: additional parameters. **a**: distal area, **b**: mesial shallow depression area, **c**: dorsal thickness, **d**: ventral thickness, **e**: distal width relative to reference line, **f**: mesial shallow depression width relative to reference line (yellow dashed line), **x**: measurement for each respective parameter. **R1**: otolith central area ratio, **R2**: otolith thickness ratio, **R3**: mesial-distal width ratio; **AP1**: incisura linea basalis width, **AP2**: mesial notch width, **AP3**: linea basalis starting point, **AP4**: central offset, **AP5**: mesial edge, **AP6**: distal edge, **AP7**: linea basalis length, **AP8**: antero-mesial projection (parameters AP1 to AP8 have been normalized according to their respective otolith length or otolith width); Abbreviations: **AR**: aspect ratio, **CI**: circularity, **EL**: ellipticity, **FF**: form factor, **OA**: otolith area (shaded in red) **OL**: otolith length, **OP**: otolith perimeter (thick blue outline), **OW**: otolith width, **RE**: rectangularity, **RL**: reference line, **RO**: roundness.

a slight protrusion, known as the postero-mesial projection (Pmp). These parameters were respectively normalized either to the otolith length (OL) or otolith width (OW) when included in statistical analyses (parameters of AP1–AP8 see Supplementary table 1).

Statistical analyses

The seventeen parameters regarding the shape indices, ratios, and normalized morphometric distances on the ventral side of the otolith (**Fig. 4, Supplementary table 1**) were treated with principal component analyses (PCA) using a correlation matrix with the aid of PAST software package (Hammer, 2023).

For further comparison, selected parameters were tested whether there were significant differences in their means/medians regarding the chosen taxa. In the case of normal distribution, parametric statistics of Student's *t*-test or Welch's *t*-test were used to compare two taxa depending on equal or unequal variances, respectively. If multiple taxa were compared, then one-way ANOVA (equal variances) or Welch's ANOVA (unequal variance) were applied followed by Tukey's pairwise test. If the data do not meet normal distribution, then non-parametric statistics Mann-Whitney test and Kruskal-Wallis analyses with Dunn's post hoc pairwise comparison were applied. For comparisons of the variance between taxa, simple F-tests or Levene tests were used. Normal distribution was checked with normal probability plots (Q-Q plots, correlation coefficient ≥ 0.95, see Supplementary table 2).

It should be noted that since there is only one sample for *B. mino*, the taxon was not included in the statistical analysis.

Results

All otoliths are bulbous and appear white. On their ventral face, they have a section that is translucent (their mesial shallow depression, including the sulculus lapilli), and the other section is opaque (the remaining area towards the distal margin). Additionally, they all have the same linea basalis (Lb) pattern as it starts from the posterior margin and goes towards the mesial margin forming the mesial notch. From there, it curves towards the distal margin slightly, and curves in the direction of the mesial margin again, forming the incisura linea basalis and it ends as it reaches the anterior margin. Selected otoliths representing each taxon are shown in Figs 5–6.

General description of otolith morphology

Based on the general appearance of the otoliths they can be separated into two main shape groups: elongated and rounded, which partly correspond to Ohe's macula- and clam-shaped grouping. Within the main shape groups, respectively two and three morpho-groups are distinguished, among which four have also been postulated by Kocsis *et al*. (2024). The "triangular", "oval", and "rectangular" shapes are classified in the elongated group, while the "circular" and "diamond" shapes are classified in the rounded group (Fig. 7).

   i. The elongated group consists of *Arius maculatus*, *A. oetik*, *A. venosus*, *Batrachocephalus mino*, *Cryptarius truncatus*, *Kyataphisa nenga*, and *Osteogeneiosus militaris.* They have no postero-mesial projection and often have their mesial and distal margins strongly angled anteriorly.
   ii. The rounded group consists of *Hexanematichthys sagor*, *Netuma bilineata, N. thalassina*, *Plicofollis argyropleuron*, and *P. nella*. These taxa have prominent postero-mesial projection (the "protrusion" just above the point where the linea basalis starts at the posterior margin) and their distal margin is symmetrically convex.

Below, the detailed descriptions of the lapillus morphologies are given for each of the studied ariid species.

Arius maculatus (n= 12) (Fig. 5, Supplementary data 5)
These lapilli have three pronounced angular-like points at the postero-mesial, antero-mesial, and antero-distal margins, making them appear triangular. Their antero-mesial projection (Amp) is subtle, and they have compact curved sulculus lapilli (Sl). Their mesial dents (Md) (the "valleys" along the outer rim of the mesial margin) are subtle, their mesial notch (Mn) is compressed, and they have deep incisura linea basalis (ILb).

Arius oetik (n= 7) (Fig. 5, Supplementary data 5)
These otoliths also appear triangular and generally quite indistinguishable from *A. maculatus*. Though, their Md appears to be more pronounced. They have subtle Amp, and compact curved Sl. Their mesial notch is compressed, and they bear shallow ILb.

Arius venosus (n= 28) (Fig. 5, Supplementary data 5)
The appearance of the otoliths is very similar to that of *A. oetik* and there are no obvious distinguishable features between the two species others than some of the *A. venosus* otoliths (n= 3) have deep bent ILb, while the others (n= 25) have shallow ILb.
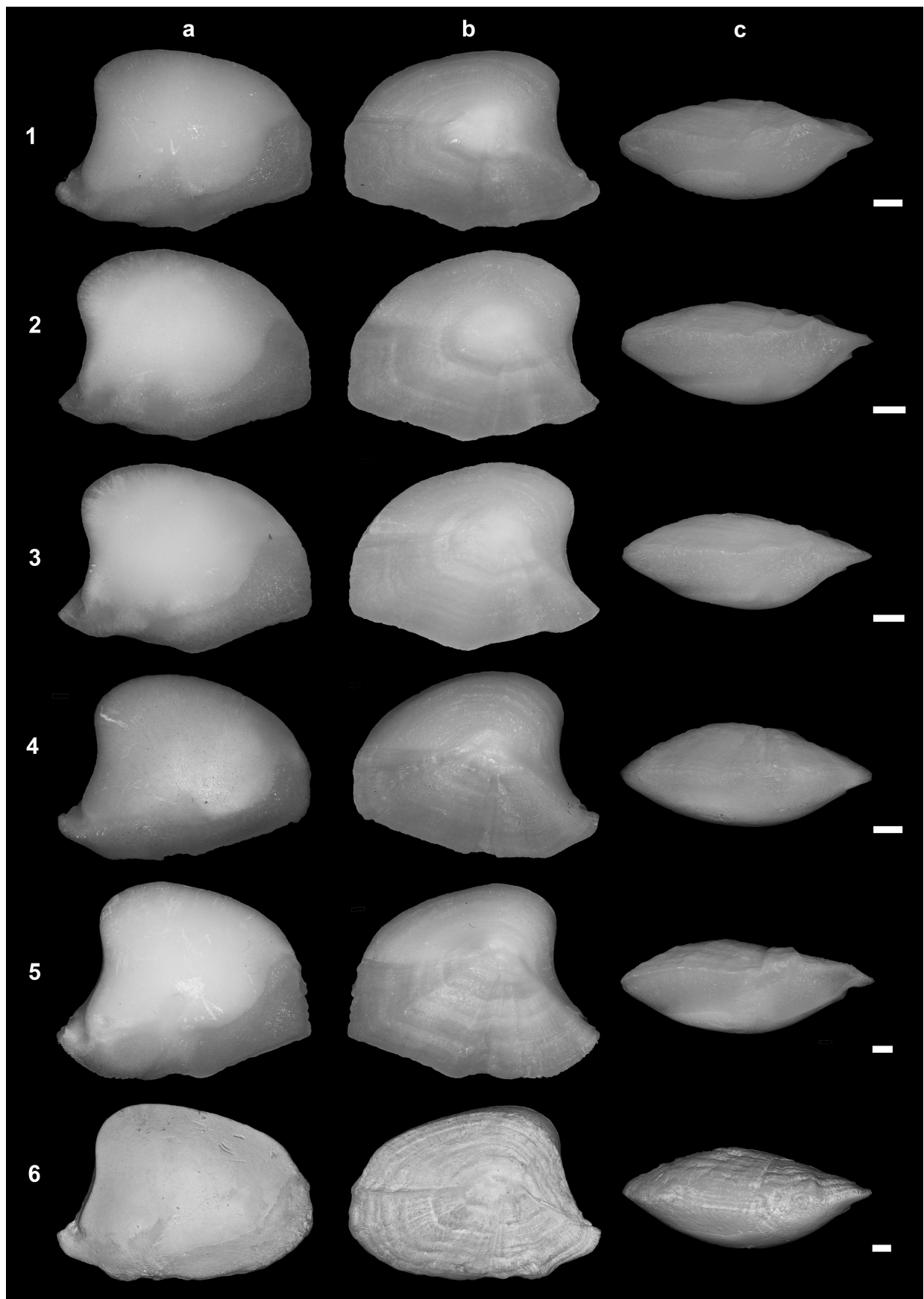
FIGURE 5. Left lapilli otolith of ariid taxa with elongated otolith. **1**: *Arius maculatus*; **2**: *Arius oetik*; **3**: *Arius venosus*; **4**: *Batrachocephalus mino*; **5**: *Cryptarius truncatus*; **6**: *Kyataphisa nenga*, **a**: Ventral view; **b**: Dorsal view; **c**: Mesial view, **Scale bar**: 1mm.
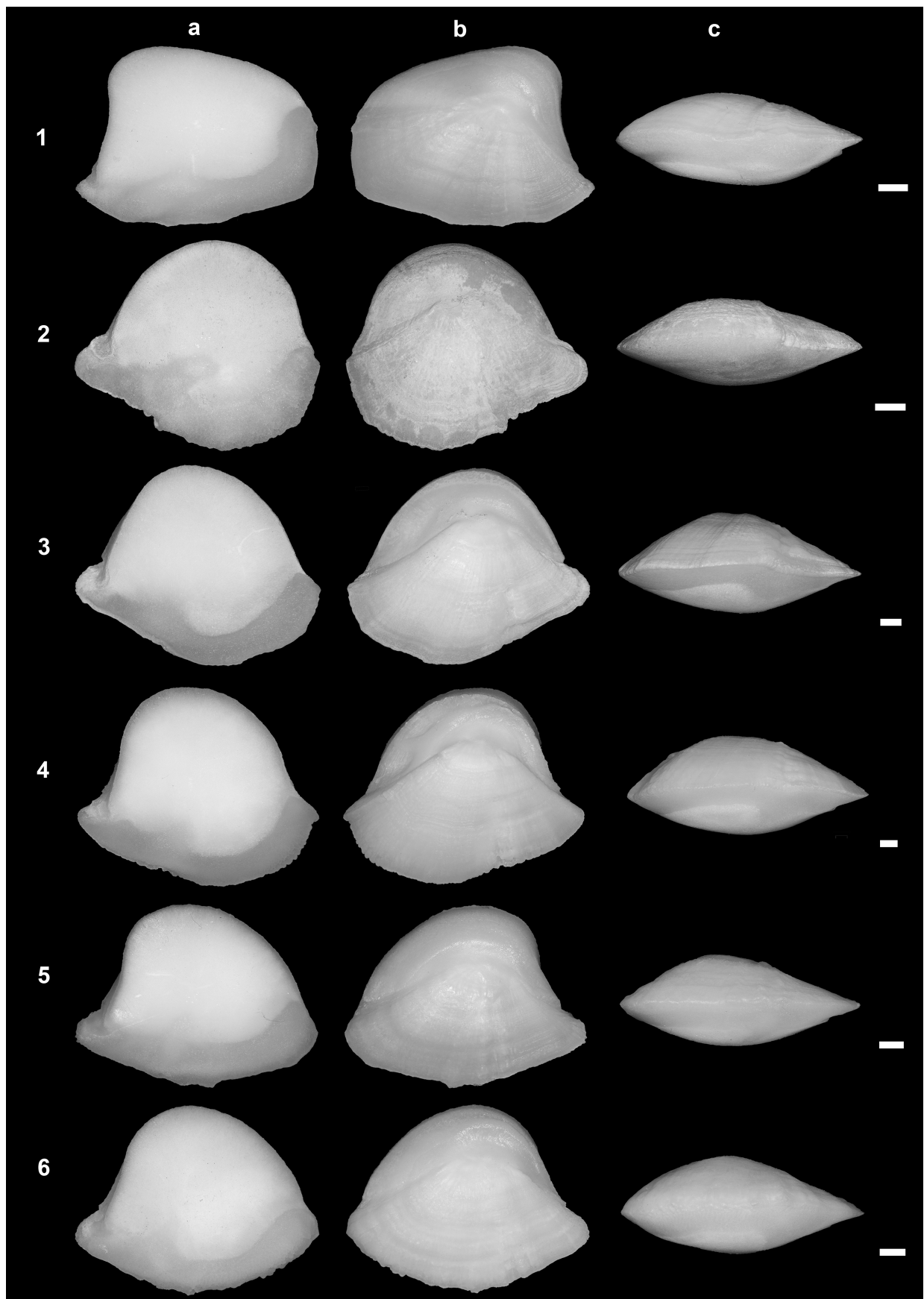
FIGURE 6. Left lapilli otolith of ariid taxa with elongated and rounded otolith. Lapillus 1 is elongated, and lapilli 2 to 6 are rounded. **1**: *Osteogeneiosus militaris*; **2**: *Hexanematichthys sagor*; **3**: *Netuma bilineata*; **4**: *Netuma thalassina*; **5**: *Plicofollis argyropleuron*; **6**: *Plicofollis nella*, **a**: Ventral view; **b**: Dorsal view; **c**: Mesial view, **Scale bar**: 1mm.
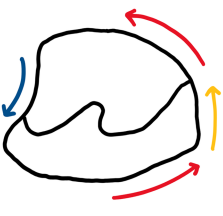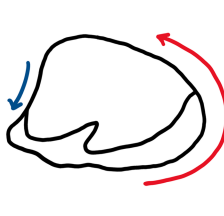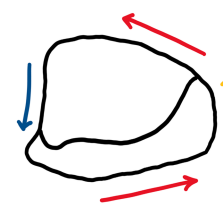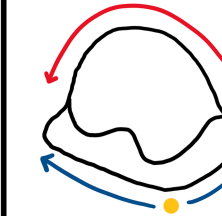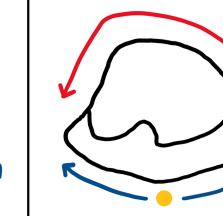
Elongated			Rounded	
Triangular shaped	Ovular shaped	Rectangular shaped	Circular shaped	Diamond shaped
A. maculatus, A. oetik, A. venosus, B. mino, and *C. truncatus*	*K. nenga*	*O. militaris*	*H. sagor, N. bilineata,* and *N. thalassina*	*P. argyropleuron* and *P. nella*

FIGURE 7. Otolith morphological characters arranged in groups and sub-groups. Arrows emphasize the shape differences between sub-groups. Colour code for the online version of the manuscript: Elongated otoliths: blue line—level of otolith's anterior curvature, red & yellow lines—roundness of the otolith's posterior end. Rounded otoliths: yellow dot—mesial apex, blue lines—lengths relative to the mesial apex, red line—distal edge roundness.

Batrachocephalus mino (n= 1) (Fig. 5, Supplementary data 5)
The otolith appears to be triangular, but it has the most compact/shortest antero-distal margin among the "triangular" shaped taxa, making it seem almost like an arrowhead. Its Amp is quite prominent. It has compact curved Sl. Its Mn is compact. It has shallow ILb.

Cryptarius truncatus (n= 22) (Fig. 5, Supplementary data 6)
The mesial shallow depression of these lapilli appears to be the widest out of all the taxa. Most of them have noticeable Md, particularly at the middle section of their mesial margin rim. Their mesial shallow depression (Msd) appears to be quite thick. Their Amp is quite prominent, and some (n= 12) have compact curved Sl, while the others (n= 10) have tubular curved Sl. They have compact Mn, and deep ILb.

Kyataphisa nenga (n= 6) (Fig. 5, Supplementary data 6)
The posterior margin of these otoliths can either be sharply or smoothly curved, but either way, they generally appear oval or egg-shaped. Their Amp is quite prominent, majority (n= 5) have compact curved Sl, with only one having tubular curved Sl. They have compact Mn and deep ILb.

Osteogeneiosus militaris (n= 14) (Fig. 6, Supplementary data 6)
These otoliths lack curvature in their general appearance, making them look rectangular-shaped. Their Amp is quite small, and they have compact curved Sl. Their Mn is very compact, and they have shallow ILb.

Hexanematichthys sagor (n= 14) (Fig. 6, Supplementary data 7)
Except for the antero-mesial margin of these otoliths, the mesial, posterior, and distal margins are well-rounded and convex. This results in a wide distal area and distal margin, and overall, makes the otoliths look circular shaped. They have wide Msd, and prominent Amp, and most (n= 8) show tubular curved Sl, while others (n= 6) have compact curved Sl. Their Mn is very prominent, and they have deeply bent ILb.

Netuma bilineata (n= 24) (Fig. 6, Supplementary data 7)
Like *H. sagor*, the curvature of most of the otoliths' margin making them appear circular. Although, the outermost part of their mesial margin is quite irregular, especially along the postero-mesial margin. Some of them (n= 8) have

prominent Md, which causes a sharp slant that makes them appear "swollen" at the postero-mesial margin. They have prominent Amp and the majority of them (n= 19) bear tubular straight Sl, while the remaining ones (n= 5) have compact straight Sl. They have prominent mesial notch and their ILb is shallow.

Netuma thalassina (n= 16) (Fig. 6, Supplementary data 7)
These otoliths share a majority of the *N. bilineata* otoliths' features, including having prominent Amp, Mn, and shallow ILb. This makes the two *Netuma* species quite indistinguishable from each other. However here, some *N. thalassina* otoliths tend to have compact straight Sl (n= 5), and most of them have compact curved Sl (n= 11).

Plicofollis argyropleuron (n= 39) (Fig. 6, Supplementary data 8)
The opaque area towards their distal margin of the otoliths appears to be narrower than that of the *Hexanematichthys* and *Netuma* genera. With the addition of their mesial margin being symmetrically convex, the otoliths appear rather diamond shaped. Their Amp is prominent, and they have tubular curved Sl. They also have compressed Mn along with deep ILb. There is very minimal variation within the samples and their appearance seem to be constant.

Plicofollis nella (n= 33) (Fig. 6, Supplementary data 8)
These lapilli are quite similar to the *P. argyropleuron*'s, in terms of the features of their mesial and distal margins, that makes them also appear diamond shaped. However, here some of the otoliths tend to have small protrusions on the outermost part of their mesial margin, typically near to the middle but slightly towards the anterior margin. They have prominent Amp and some of them have tubular curved Sl (n= 22), and others are compactly curved (n= 11). Their Mn appears slightly compressed, and a few have shallow ILb (n= 13), while the remaining have deep ILb (n= 20).

Otolith morphometric data

Otolith density (OD), mass (OM), and volume (OV) exhibit similar characteristics, all increasing linearly with otolith size (*e.g.*, Fig. 8).

Principal component analyses (PCA) were then applied to the 17 parameters which yielded eigenvalues where the first three PCs explain 72 % of all the variances among the samples (Fig. 9). Regarding the parameters, many of them display strong correlations. For example, form factor (FO) and roundness (RO) are very strongly positively correlated, while both have a very strong negative correlation with circularity (CI) (Pearson $r^2 >0.9$) (Fig. 9B). Similarly, aspect ratio (AR) and ellipticity (EL), or AP2 and AP3 parameters have very strong positive correlations, while AP7 and AP8 have very strong negative correlations. Another example is rectangularity (RE), which is strongly correlated ($r^2 = 0.75–0.9$) with many parameters like positively to AP2, AP3, AP7, while negatively to R2, R3, and AP8 (Fig. 9B). It is clear that some of these parameters express very similar or opposing morphological traits, and the number of parameters may be reduced for further statistical comparisons.

Nevertheless, along the PC1, two evident otolith groups can be distinguished, which are mainly pulled by parameters of RE, AP2, AP3 in positive and R2, R3, AP8 in negative directions. The first group includes *Hexanematichthys sagor, Netuma bilineata, N. thalassina, Plicofollis argyropleuron* and *P. nella*, and the second have *Arius maculatus*, *A. oetik*, *A. venosus*, *Batrachocephalus mino*, *Cryptarius truncatus*, *Kyataphisa nenga*, and *Osteogeneiosus militaris*. These two groups confirm the previous separation of the otoliths (Fig. 7) and therefore they are referred further in the text to rounded and elongated groups, respectively. Parameters like rectangularity (RE) or mesial-distal width ratio (R3) are key morphological parameters to separate these groups (Fig. 10 A–D), however, cross-plots between selected parameters could also reveal additional subtle differences within the two groups (Fig. 10 E–F).

Further statistical analyses are considered separately for the elongated and rounded morpho-groups. The 17 parameters (Fig. 4) for all the individual ariid taxa were tested for normal distribution with Q-Q plots and many of them yielded correlation coefficients higher than 0.95 (Supplementary table 2). For these, parametric tests (Student's *t*-test or Welch's *t*-test and one-way ANOVA (equal variances) or Welch's ANOVA (unequal variance), along with Tukey's pairwise test) were applied to trace whether there are significant differences among the taxa, while those where normal distribution did not meet non-parametric test were used for this purpose (*e.g.*, Kruskal-Wallis test with Dunn's post hoc pairwise comparisons).
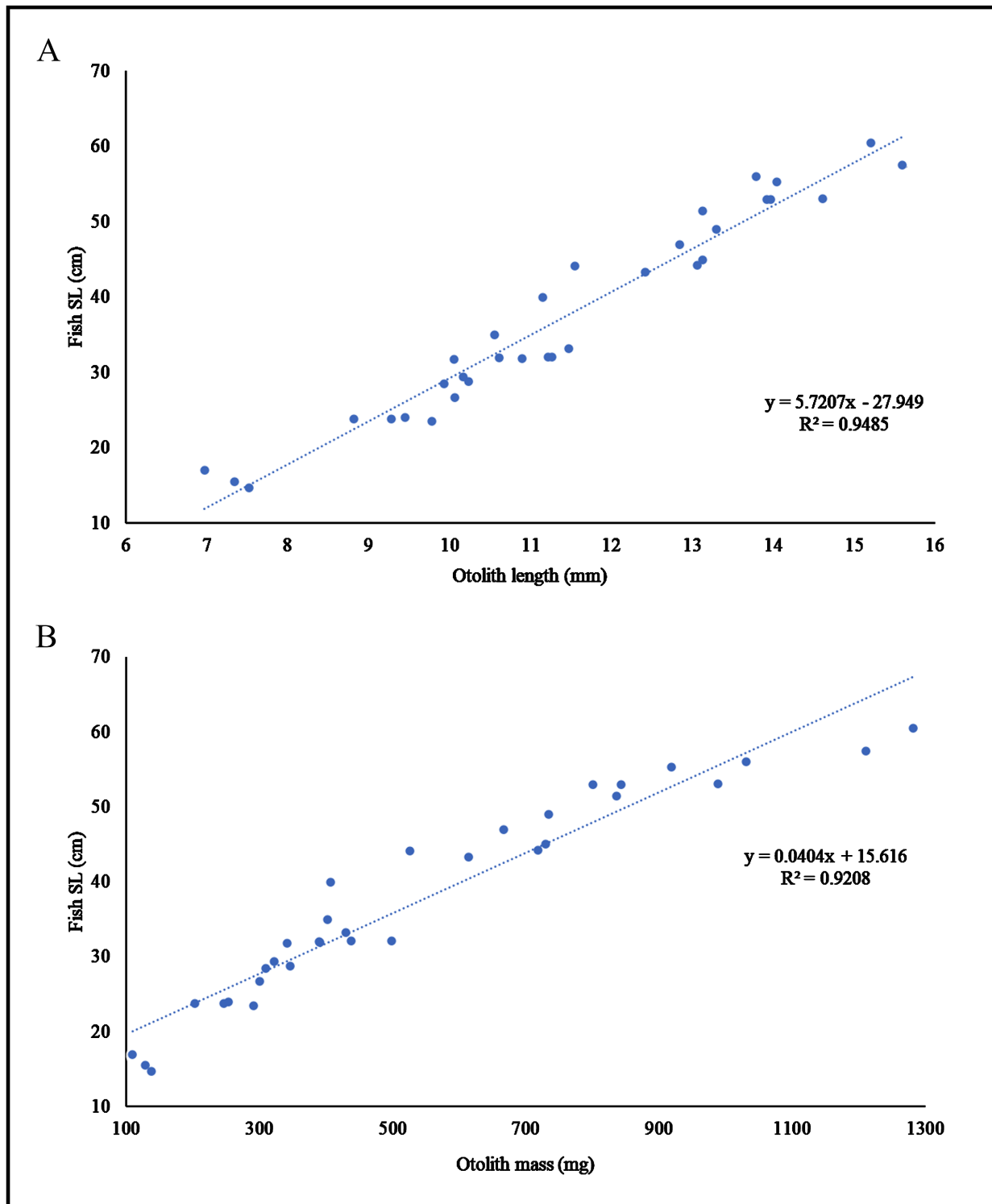
FIGURE 8. An example of two different allometric graphs for an Ariidae taxon (*Plicofollis nella*). **A**: fish standard length vs otolith length, **B**: fish standard length vs. otolith mass.
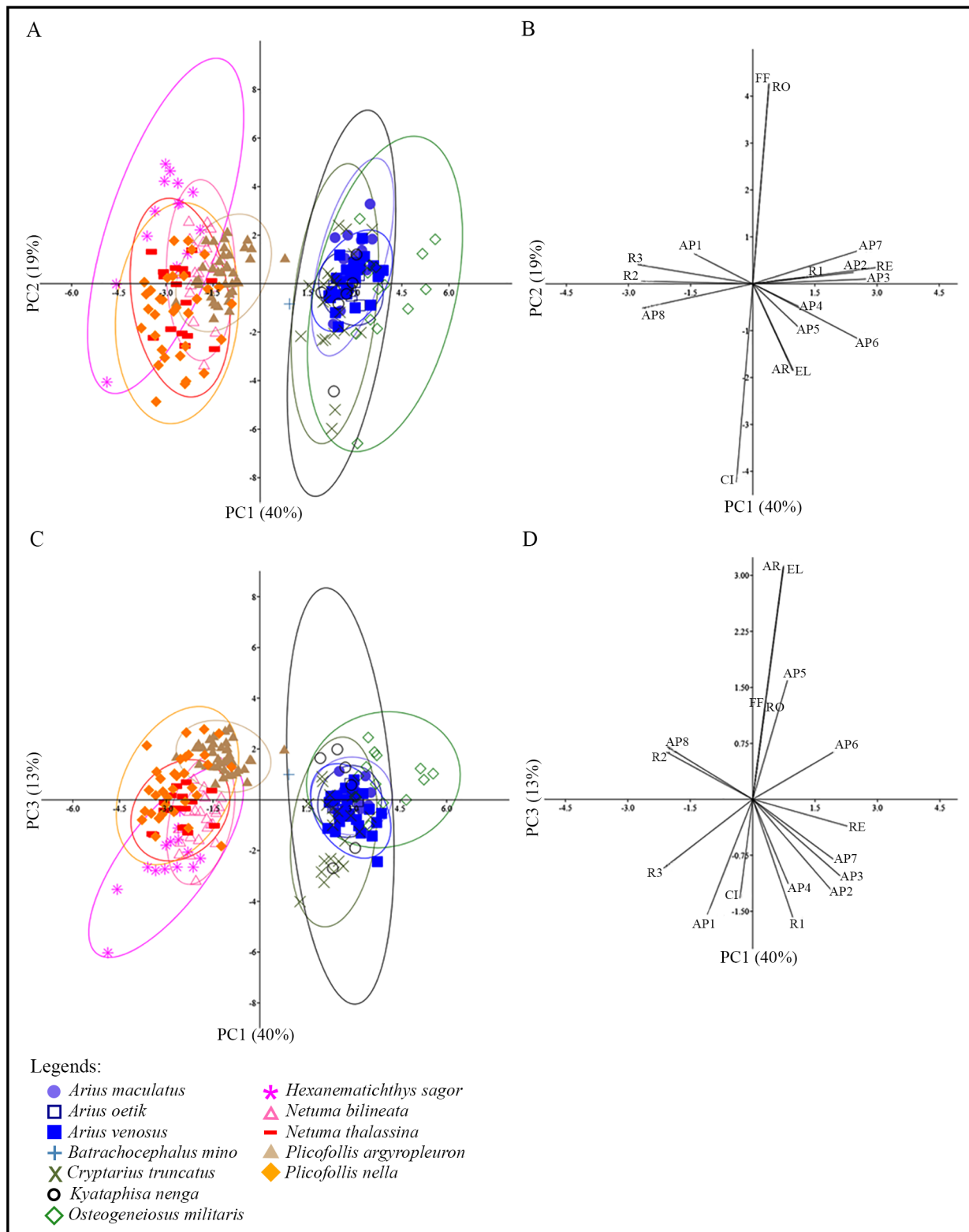
FIGURE 9. Scatter plots and biplots of principal component analyses (PCA). **A&B**: PC 1 vs. PC 2, **C&D**: PC 1 vs. PC 3, **A&C**: Scatter plots, **B&D**: Biplots.

Discussion

Principal Component Analysis (PCA) identified two major morphological groups based on otolith shape: one with elongated features and one with a more rounded form. These groupings are supported by parameters such as rectangularity (RE), mesial-distal width ratio (R3), the width associated with the linea basalis starting point (AP3), and the length corresponding to the otolith distal edge (AP6) (Fig. 10). Significant differences were found based on Student's t-test (*e.g.*, RE: $t_{(214)} = 33.7$, $p < 0.01$; R3: $t_{(214)} = 25.19$, $p < 0.01$; see Supplementary table 3), allowing for a more detailed investigation of the elongated and rounded otoliths within their respective groups.

Subsequently, further comparisons were conducted using boxplots of selected parameters, and the differences in means among the taxa are discussed below (see Supplementary tables 4–5 for precise values). For both pairwise and multi-taxa comparisons, the null hypothesis posited no statistical difference in the mean or median of a given variable among the taxa. Following assessments for normality (Supplementary table 2) and variance comparisons, appropriate statistical tests were applied. When the p-value was less than 0.05, the null hypothesis was rejected, indicating a statistically significant difference.
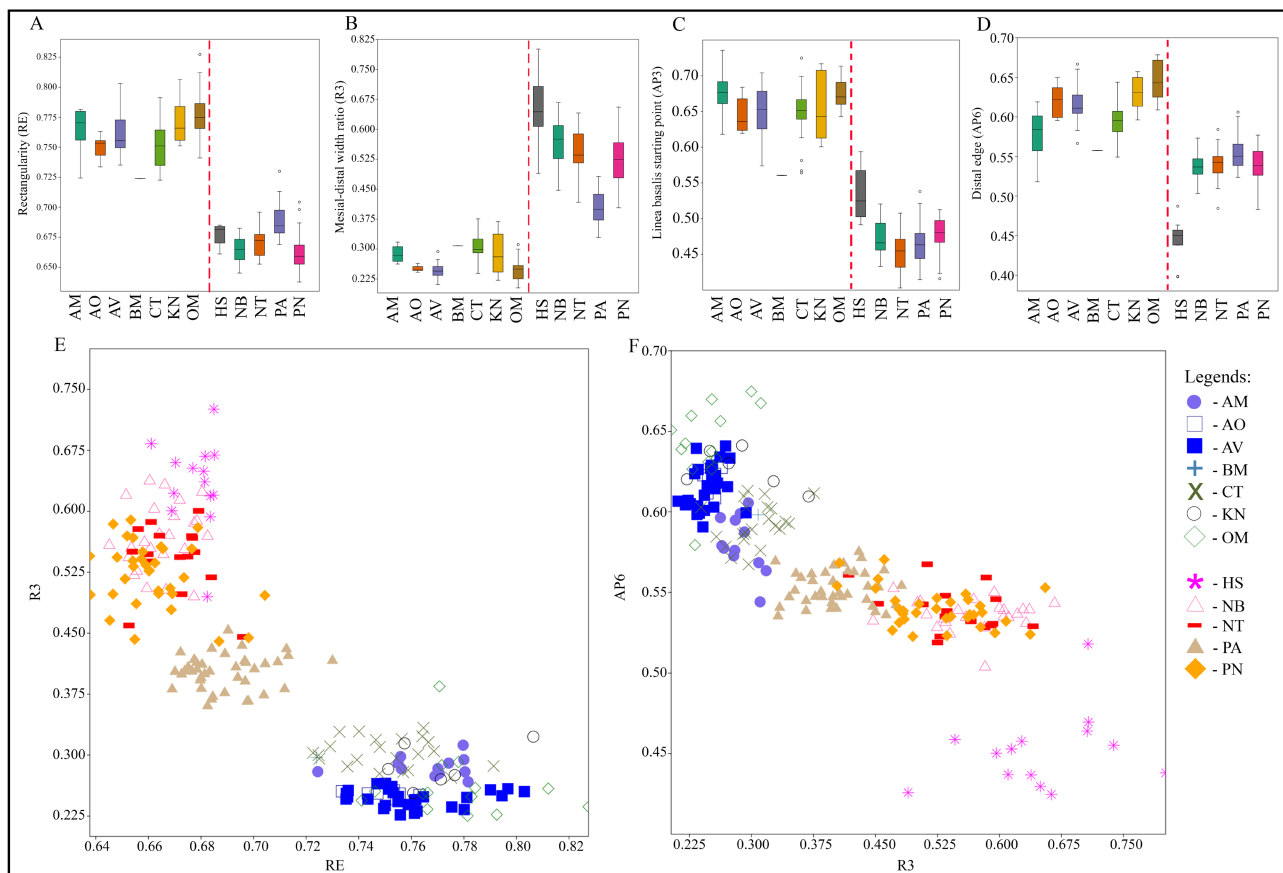

FIGURE 10. Boxplots and cross-plots for selected parameters with strong correlation. The dotted line in the middle of each boxplot separates the elongated (right) and rounded (left) groups. Small white dots within the boxplots indicate outliers**. A–D:** Boxplots, **E&F:** XY graphs; **AM**: *Arius maculatus*, **AO**: *Arius oetik*, **AV**: *Arius venosus*, **BM**: *Batrachocephalus mino*, **CT**: *Cryptarius truncatus*, **KN**: *Kyataphisa nenga*, **OM**: *Osteogeneiosus militaris*, **HS**: *Hexanematichthys sagor*, **NB**: *Netuma bilineata*, **NT**: *Netuma thalassina*, **PA**: *Plicofollis argyropleuron,* **PN**: *Plicofollis nella*.

Elongated group

For this group, the shape indices did not present any obvious separation among the taxa. However, within the *Arius* genera, circularity (CI) (Fig. 11A), format factor (FF)**,** and roundness (RO) showed some degrees of separation between *A. maculatus* and the other two *Arius* species. Note that FF & RO express very similar morphometric variation (see Fig. 9B), therefore only one of them is shown here on boxplots (Fig. 11B). Levene's test yielded
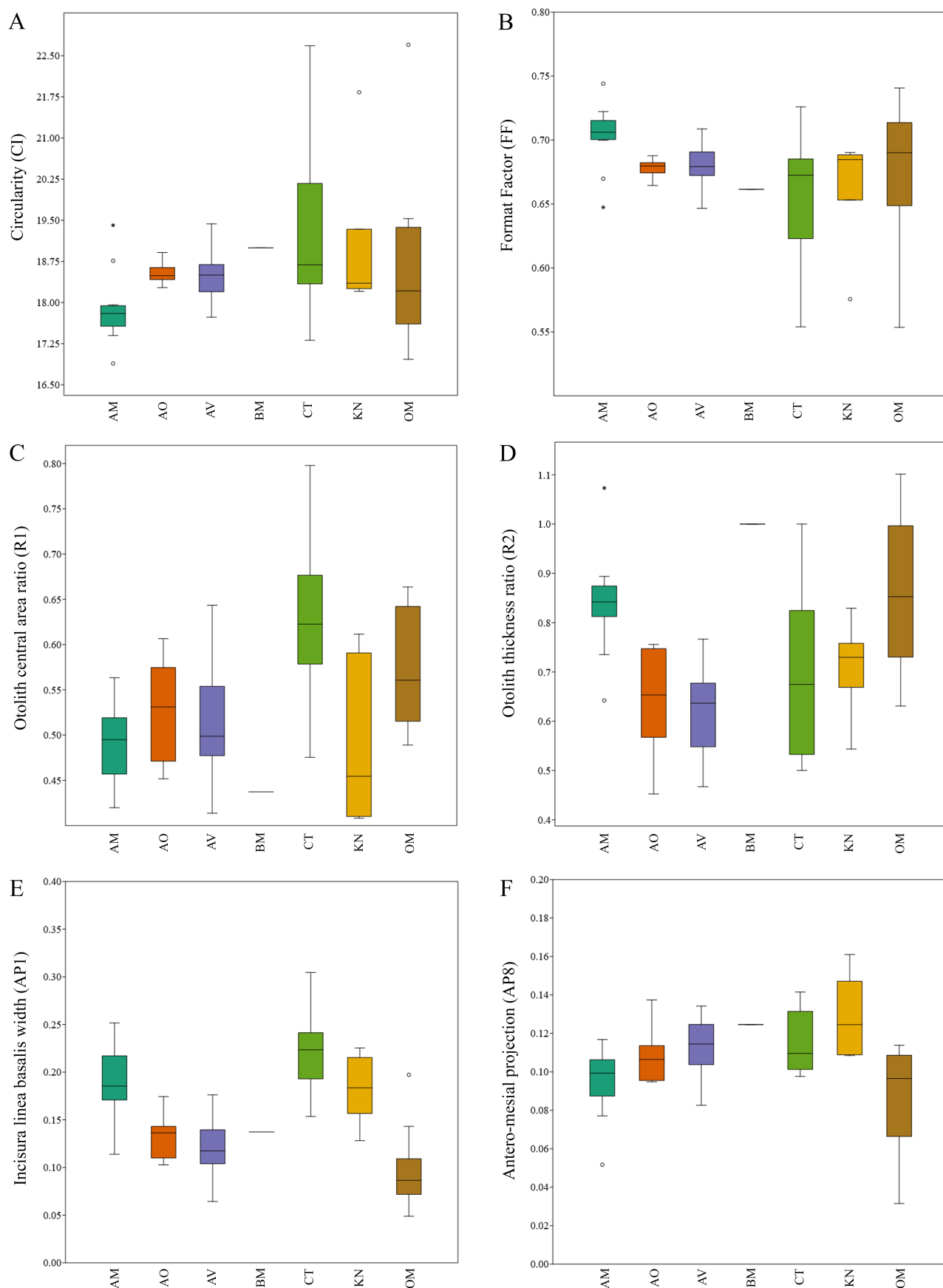
FIGURE 11. Boxplots with parameters that are useful for differentiating ariid taxa classified in the elongated group. **AM**: *Arius maculatus*, **AO**: *Arius oetik*, **AV**: *Arius venosus*, **BM**: *Batrachocephalus mino*, **CT**: *Cryptarius truncatus*, **KN**: *Kyataphisa nenga*, **OM**: *Osteogeneiosus militaris*.

equal variance for all three parameters (CI–$F_{(2, 44)}$ = 7.76, p = 0.18, FF–$F_{(2, 44)}$ = 8.41, p = 0.15, RO–$F_{(2, 44)}$ = 8.45, p = 0.16). Since the parameters did not show normal distribution in the case of *A. maculatus,* Kruskal-Wallis test was used, which revealed a significant difference (CI-$H_{(2)}$ = 11.14, p < 0.01, FF-$H_{(2)}$ = 11.05, p < 0.01, RO-$H_{(2)}$ = 11.07, p < 0.01). Their corresponding Dunn's post-hoc pairwise test showed that *A. maculatus* has p-values less than 0.05 when compared to the other *Arius* species for all three parameters, validating significant differences.

For the otolith central area ratio (R1), *C. truncatus* seemed to be on the higher end of the group (Fig. 11C). The Levene's test revealed equal variance among the taxa ($F_{(5, 83)}$ = 13.28, p = 0.22), and their Kruskal-Wallis test suggested at least one of the taxa with statistically different mean from the others ($H_{(5)}$ = 37.35, p < 0.01). The resulting Dunn's post-hoc pairwise test showed a significant difference when *C. truncatus* was compared with the other taxa (except *O. militaris*) within the group, which supports the observation of *C. truncatus* having the thickest mesial shallow depression.

In general, the boxplot for otolith thickness ratio (R2) (Fig. 11D) indicated that the taxa within the elongated group have a thicker ventral face in mesial view. The Levene's test revealed unequal variance between the taxa of the group ($F_{(5, 83)}$ = 10.79, p < 0.01). The Kruskal-Wallis tests suggested statistical difference ($H_{(5)}$ = 33.75, p < 0.01), and the resulting Dunn's post-hoc pairwise test revealed that *A. maculatus* and *O. militaris* are significantly different from the other taxa, but not from *K. nenga* and from each other.

Out of the eight additional parameters, the boxplots for incisura linea basalis width (AP1) (Fig. 11E), distal edge (AP6) (Fig. 10D), and antero-mesial projection (AP8) (Fig. 11F) seemed to be the most discriminative for the elongated group. The Levene's test for the group's AP1 revealed equal variance among the taxa ($F_{(5, 83)}$ = 36.88, p = 0.73), meanwhile the Q-Q plot indicated normal distribution for most of the taxa except OM. Therefore, the Kruskal-Wallis test was computed, which yielded significant differences among the taxa in the group ($H_{(5)}$ = 61.41, p < 0.01). Their corresponding Dunn's post-hoc pairwise test revealed significant differences between some of the taxa, particularly separating *A. oetik*, *A. venosus*, and *O. militaris* from the other taxa within the group.

The AP6 boxplot generally suggested that their distal margin is slightly slanted towards the anterior margin when compared with the rounded group. The Levene's test showed equal variance among the taxa ($F_{(5, 83)}$ = 13.93, p = 0.57), while they are statistically different according to one-way ANOVA test ($F_{(5, 83)}$ = 13.93, p < 0.01). Tukey's pairwise test indicated that, *A. maculatus* is significantly different from the other taxa (except *C. truncatus*), while *O. militaris* is statistically different from the others except of *A. oetik* and *K. nenga*.

Regarding the AP8, the boxplot showed *O. militaris* having the lowest range of values, and slightly separated from the other elongated taxa. The Levene's test suggested equal variance ($F_{(5, 83)}$ = 7.07, p = 0.28). As many of the taxa have low correlation coefficients on a Q-Q plot, the Kruskal-Wallis test is used, which indicated a significant difference among the taxa ($H_{(5)}$ = 23.04, p < 0.01). The p-values of their Dunn's post-hoc pairwise roughly demonstrated the slight separation of *O. militaris* from the others.

Overall, the morphometrical analysis within the elongated group can confidently separate the *Arius* genera from the other taxa based on the parameters of CI, FF, and RO. Although, it becomes quite ineffective when all the taxa are considered.

Rounded group

For the rounded group, there seemed to be minor separation observed within aspect ratio (AR) and ellipticity (EL) (Fig. 12A) (both parameters showed similar distribution in their boxplots, see also Fig. 9B). The Levene's test revealed unequal variances among the taxa (AR -$F_{(4, 121)}$ = 29.69, p < 0.01, and EL -$F_{(4, 121)}$ = 31.03, p < 0.01), which explains the distribution and spread of data in their respective boxplots. Because the data are normally distributed for all the taxa, Welch's ANOVA test was assessed, and the resulting data yielded significant difference in the mean for AR and EL (AR-$F_{(46.63)}$ = 47.65, p < 0.01 and EL-$F_{(45.77)}$ = 46.32, p < 0.01). A majority of the group's Tukey's pairwise test for both AR and EL has p-values below 0.05, especially *H. sagor* and *P. argyropleuron*, which each show significant differences from other rounded taxa. Since AR and EL reflect the level of "elongation" of the otoliths and *H. sagor* has the least value for both, it can be stated that this species' otolith is the most rounded of all.

Looking at the boxplot for the group's RE (Fig. 10A), *P. argyropleuron* is slightly separated from the other taxa. A Levene's test suggested equal variance ($F_{(4, 121)}$ = 25.44, p = 0.16), while the Kruskal-Wallis test showed significant differences among the taxa ($H_{(4)}$ = 61.17, p < 0.01). Dunn's post-hoc pairwise test supports significant separation

of *P. argyropleuron* from most of the other taxa. This is reasonable as morphologically the taxon does appear to be the least rounded.

Boxplots for R1 (Fig. 12B) revealed that *H. sagor* has the highest value within the rounded group. Q-Q plots indicate normal distribution for all the taxa, while Levene's test showed unequal variance ($F_{(4, 121)} = 26.49$, $p < 0.01$). Therefore Welch's ANOVA test was used and yielded significant differences ($F_{(46.73)} = 22$, $p < 0.01$). Tukey's pairwise test revealed further details according to which the *H. sagor* and *N. thalassina* are statistically different from the other taxa and from each other. Therefore, it points to that *H. sagor* has the widest mesial shallow depression, while *N. thalassina* has the narrowest one.

The boxplot of the R3 parameter (Fig. 10B) showed that *H. sagor* has the highest readings, while *P. argyropleuron* has the lowest one. The Levene's test indicated that there are slightly equal variances among the taxa ($F_{(4, 121)} = 64.77$, $p = 0.053$), while correlation coefficients of the Q-Q plots reflect normal distribution ($R^2 > 0.95$). The corresponding one-way ANOVA test resulted in significant differences among them ($F_{(4, 121)} = 64.77$, $p < 0.01$), meanwhile Tukey's pairwise test separates these two species with significant differences from the rest of the group. This also indicates that within the rounded group, relative to the reference line, *H. sagor* generally has the widest mesial measurement, while *P. argyropleuron* has the narrowest one.
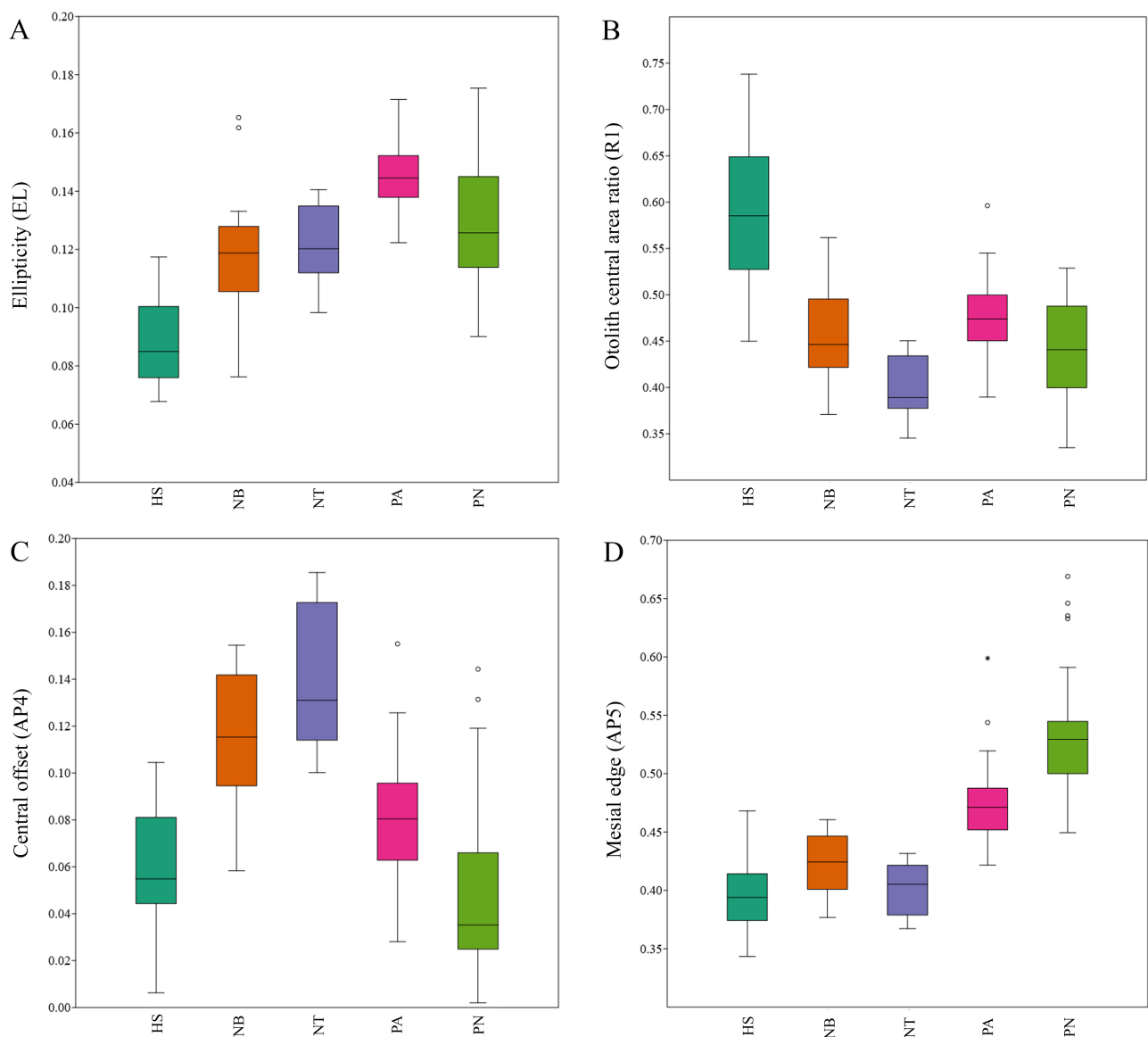

FIGURE 12. Boxplots with parameters that are useful for differentiating ariid taxa classified in the rounded group. **HS**: *Hexanematichthys sagor*, **NB**: *Netuma bilineata*, **NT**: *Netuma thalassina*, **PA**: *Plicofollis argyropleuron*, **PN**: *Plicofollis nella*.

Parameters relating to otolith length such as central offset (AP4) (Fig. 12C), mesial edge (AP5) (Fig. 12D), and distal edge (AP6) (Fig. 10D) appear to be the most advantageous for distinguishing the taxa within the rounded group. Starting with AP4, the Levene's test indicated that the spread of values is approximately the same across taxa ($F_{(4, 121)}$ = 31.93, p = 0.21), meanwhile the data are normally distributed. This prompted for a one-way ANOVA test, which showed significant difference ($F_{(4, 121)}$ = 31.93, p < 0.01). The resulting Tukey's pairwise test denote that the two *Netuma* species are significantly different from the other taxa but not from each other. An F test was then computed for comparing the variances of *N. bilineata* and *N. thalassina*, that showed equal variance ($F_{(38)}$ = 1.14, p = 0.76). Their corresponding Student's *t*-test reflect sufficient evidence to reject the null hypothesis, as their means are significantly different ($t_{(38)}$ = 2.87, p < 0.01).

The Levene's test for AP5, showed unequal variances among the group's taxa ($F_{(4, 121)}$ = 61.06, p = 0.017), but the data is not normally distributed for *P. argyropleuron* (Q-Q plot R^2 < 0.95). Therefore, a Kruskal-Wallis test was applied with the result of significantly different medians between the taxa ($H_{(4)}$ = 95.28, p < 0.01). Dunn's post-hoc pairwise test revealed that the *Plicofollis* genus have p-values less than 0.05 when compared to each other and with the other genera of the group, confirming their statistically significant differences. AP5 can be further indicative for the *Hexanematichthys* and *Netuma* having protrusion more on the posterior side of their mesial margin.

In the boxplot of AP6 (Fig. 10D), *H. sagor* has the lowest values and can be strongly separated from all the other rounded taxa. This is also the only taxon that is not normally distributed. The Levene's test revealed equal variances ($F_{(4, 121)}$ = 75.07, p = 0.49), while the corresponding Kruskal-Wallis test then yielded significant difference ($H_{(4)}$ = 47.23, p < 0.01). The following Dunn's post-hoc pairwise test confirms the observation of the boxplot with such as the *H. sagor* (p < 0.05) is significantly different from the other members of the group. The result also implies that *H. sagor* has the most symmetrical distal margin.

Overall, the morphometric tests seem to be the most effective for differentiating the taxa within the rounded group, and *H. sagor* is the most distinct among them.

Proposed guideline for ariid taxa identification

The first step for separating the ariid taxa is sorting them for their respective general shape of elongated or rounded group. This can be assessed by the parameters of RE, R3, AP3, and AP6. The taxa within each group can then be further identified following the list below:

Elongated group:
  i.   Within the *Arius* genus, parameters CI, FF, and RO are especially useful for distinguishing *A. maculatus* from *A. oetik* and *A. venosus*, however they are not helpful when comparing them with other taxa in the group.
  ii.   Parameter R1 is particularly useful for distinguish *C. truncatus*.
  iii. The parameters of R2, AP1, AP6, and AP8 can separate *O. militaris* from most of the taxa in the group. The parameters are also simultaneously useful for grouping the ariid taxa into the "rectangular shape" morpho-group (Fig. 7).

Rounded group:
  i.   *H. sagor* can be isolated from the other taxa by evaluating the parameters of AR, EL, R1, R3, and especially AP6.
  ii.   Parameter AP4 is particularly useful for distinguishing the *Netuma* genus as whole, and even between two species of *N. thalassina* and *N. bilineata*.
  iii. *N. thalassina* is specifically separated from the other taxa by parameter R1.
  iv.   The parameter AP5 is useful separating the *Plicofollis* genus from the others. This also means, the parameter is valuable for separating the morpho-groups of "circular" and "diamond shaped" (Fig. 7).
  v.   *P. argyropleuron* can be distinguished by evaluating parameters AR, EL, RE, and R3.

It should be noted that this guideline is not definitive, and could change when other Ariidae taxa that are not included in this study are involved in future.

Insights to variation in otolith morphology and recommendations for improvement

It is important to note that the size of the otolith does not necessarily follow the fish size, i.e., small fish species can have large otoliths, while big fish species can possess small otoliths (Weisler, 1993). Although, otolith growth has a strong correlation with fish growth (see Fig. 8), variables relating to otolith size (otolith length and otolith mass) are roughly proportional to the somatic growth of the fish, and it remains true for all ariid taxa. The morphometric data showed statistically significant differences among some of the taxa, suggesting that it is unlikely that the observed relationships occur as a result of random chance. Still, the overall results convey limited differentiation, especially within the elongated group. This is best explained by intraspecific variations within the ariid species, together with limited interspecific differences.

This was expected, as although otolith shape is determined during early life stages, particularly when the fish is still living in the estuary (Vignon, 2012), genetics often influence the heritability of certain traits, and allometric growth typically causes variation in otolith morphology (Chen & Zhu, 2023). These variations can diminish the precision of morphometric data and compromise the accuracy of species identification (Santos & Vaz-dos-Santos, 2023).

Environmental factors, including biotic (*e.g.*, food availability) and abiotic (*e.g.*, depth, temperature, salinity), influence otolith features, including growth patterns, chemical composition, and particularly shape (Gauldie & Crampton, 2002; Mahé *et al.* 2019). Interestingly, the fish total length (TL) range for the taxa within the elongated group are generally smaller than those in the rounded group (fish TL within elongated group: 16–42.5 cm, within rounded group: 17.5–91 cm). The diet and habitat preference of the studied ariid species does not differ too much from each other as they tend to inhabit a mixture of both marine and brackish waters including coastal waters, estuaries, and tidal reaches of rivers (Froese & Pauly, 2024; Kailola, 1999). For example, the taxon *N. thalassina* mostly inhabits marine waters, while *C. truncatus* typically live under brackish conditions (Marceniuk & Menezes, 2007). The tropical climate of the Borneo region brings minimal seasonal changes, even so, the alternating wet and dry season can still affect the ecological properties (such as salinity) of the Bornean waters. Since many of the ariids are well-adapted for changing salinity, the morphological differences of otoliths within the studied ariid taxa are quite likely affected mainly by biological processes than environmental factors.

Since most fish samples were obtained from wet markets without precise catch location data, uncertainties arise, including batches of fish might have been caught across different locations on the same day. Future studies on ariid otoliths should incorporate more precise locality data regarding fish origin. Moreover, recording additional parameters, such as weight, gender, and otolith appearance at different life stages (juvenile vs. adult), could significantly enhance the analysis. Morphometric data of the features found on the dorsal face of the otolith can give further understanding on variation of otolith morphology within a species and could produce more effective morphometric separation. Adding more parameters and exploring alternative measurements can possibly enhance morphometric results, providing more comprehensive descriptions.

Conclusion

The updated ariid otolith terminologies and newly defined features demonstrate the importance of detailed morphological descriptions in uncovering subtle interspecific and intergeneric differences among lapillus otoliths. By converting otolith shape and appearance into quantitative morphometric data, our statistical analyses—incorporating techniques such as Principal Component Analysis, *t*-tests, and boxplot comparisons—have significantly enhanced our ability to discern both similarities and differences among closely related ariid taxa. Notably, the taxonomic relevance of this approach was most pronounced within the rounded group, where parameters such as aspect ratio, incisura linea basalis width, and otolith central area ratio consistently enabled clear differentiation at the genus and, in some cases, species levels. Although the elongated group presented greater challenges due to overlapping morphological traits, differences in parameters such as rectangularity and mesial-distal width ratio indicate promising avenues for further refinement. Moreover, the integration of these morphometric techniques with other morphological and ecological data holds considerable potential for advancing our understanding of ariid systematics and evolutionary history. Overall, while limitations remain in achieving fine-scale taxonomic resolution, this study demonstrates that lapillus otolith morphological analysis represents a valuable supplementary tool for the systematic study of ariid fishes and may inform taxonomic revisions in other teleost groups as well.

Acknowledgements

References

Abdurahman, S.W., Ambak, M.A., Sheriff, S.M., Mohamed, S.Y.A.A. & Chowdhury, A.J.K. (2016) Morphological variations of *Plicofollis* species (Siluriformes: Ariidae) in Peninsular Malaysia: An insight into truss network approach. *Sains Malaysiana*, 45 (1), 1–7.

Acero, P.A. (2002) Order Siluriformes-Ariidae. *In*: *The living marine resources of the western central Atlantic*. FAO, Rome, pp. 831–852.

Acero, P.A. & Betancur-R, R. (2007) Monophyly, affinities, and subfamilial clades of sea catfishes (Siluriformes: Ariidae). *Ichthyological exploration of freshwaters*, 18 (2), 133.

Aguilera, O.A., Moraes-Santos, H., Costa, S., Ohe, F., Jaramillo, C. & Nogueira, A. (2013) Ariid sea catfishes from the coeval Pirabas (Northeastern Brazil), Cantaure, Castillo (Northwestern Venezuela), and Castilletes (North Colombia) formations (early Miocene), with description of three new species. *Swiss Journal of Palaeontology*, 132 (1), 45–68.
https://doi.org/10.1007/s13358-013-0052-4

Aguilera, O., Lopes, R.T., Rodriguez, F., dos Santos, T.M., Rodrigues-Almeida, C., Almeida, P., Machado, A.S. & Moretti, T. (2020) Fossil sea catfish (Siluriformes; Ariidae) otoliths and in-skull otoliths from the Neogene of the Western Central Atlantic. *Journal of South American Earth Sciences*, 2020, 102619.
https://doi.org/10.1016/j.jsames.2020.102619

Arroyo-Zúñiga, K.I., Pacheco-Ovando, R., Granados-Amores, E., Granados-Amores, J., González Ramírez, J. & Díaz-Santana-Iturrios, M. (2022) Lapillus otolith shape, a useful taxonomic feature for the identification of sea catfishes (Ariidae: Siluriformes) from the north-eastern Pacific. *Journal of Fish Biology*, 101 (5), 1262–1269.
https://doi.org/10.1111/jfb.15198

Betancur-R, R. (2009) Molecular phylogenetics and evolutionary history of ariid catfishes revisited: A comprehensive sampling. *BMC Evolutionary Biology*, 9 (1), 175.
https://doi.org/10.1186/1471-2148-9-175

Bond, C.E. (1996) *Biology of Fishes. 2nd Edition*. Saunders College Publisher, Fort Worth, Texas, 750 pp.

Burgess, W.E. (1989) An atlas of freshwater and marine catfishes. A preliminary survey of the Siluriformes. *TFH Publication, Neptune City, Canada*, 28, 305–325.

Chen, Y. & Zhu, G. (2023) Using machine learning to alleviate the allometric effect in otolith shape-based species discrimination: the role of a triplet loss function. *ICES Journal of Marine Science*, 80 (5), 1277–1290.
https://doi.org/10.1093/icesjms/fsad052

Dantas, D.V., Barletta, M., Costa, M.F., Barbosa-Cintra, S.C.T., Possatto, F.E., Ramos, J.A., Lima, A.R. & Saint-Paul, U. (2010) Movement patterns of catfishes (Ariidae) in a tropical semi-arid estuary. *Journal of Fish Biology*, 76 (10), 2540–2557.
https://doi.org/10.1111/j.1095-8649.2010.02646.x

Farooq, N. & Panhwar, S.K. (2023) Taxonomic and Otolith Shape Parameters of Nine Sympatric Catfishes Commercially Harvested in Pakistan. *Croatian Journal of Fisheries*, 81 (1), 23–32.
https://doi.org/10.2478/cjf-2023-0003

Ferraris, C.J. (2007) Checklist of catfishes, recent and fossil (Osteichthyes: Siluriformes), and catalogue of siluriform primary types. *Zootaxa*, 1418 (1), 1–628.
https://doi.org/10.11646/zootaxa.1418.1.1

Froese, R. & Pauly, D. (Eds.) (2024) FishBase. Version February 2024.World Wide Web electronic publication. Available from: https://www.fishbase.org (accessed 25 April 2025)

Gauldie, R.W. & Crampton, J.S. (2002) An eco-morphological explanation of individual variability in the shape of the fish otolith: comparison of the otolith of *Hoplostethus atlanticus* with other species by depth. *Journal of Fish Biology*, 60 (5), 1204–1221.
https://doi.org/10.1006/jfbi.2002.1938

Hammer, Ø. (2023) PAST - PAleontological Statistics. Version 4.13, Reference manual. (PDF). Available from: https://www.

fileeagle.com/software/download/16046/e249bd (accessed 10 May 2023)

Kailola, P.J. & Bussing, W.A. (1995) *Ariidae (frecuentemente 'Tachysuridae' en la literatura)*. *In*: Fischer, W., Krupp, F., Schneider, W., Sommer, C., Carpenter, K.E. & Niem, V.H. (Eds.), *Guia FAO para la identificacion de especies para los fines de la pesca. Pacific centro-oriental. Vol. II. Vertebrados. Parte I*. Food and Agriculture Organisation, Rome, pp. 860–886.

Kailola, P.J. (1999) Order Siluriformes Ariidae. *In*: Carpenter, K.E. & Niem, V.H. (Eds.), *The Living Marine Resources of the Western Central Pacific*, 3, pp. 1827–1847.

Kocsis, L., Lin, C.H., Bernard, E. & Johari, A. (2024) Late Miocene teleost fish otoliths from Brunei Darussalam (Borneo) and their implications for palaeoecology and palaeoenvironmental conditions. *Historical Biology*, 36 (12), 2642–2676.
https://doi.org/10.1080/08912963.2023.2271489

Maciel, T.R., Vaz-dos-Santos, A.M., Barradas, J.R.D.S. & Vianna, M. (2019) Sexual dimorphism in the catfish *Genidens genidens* (Siluriformes: Ariidae) based on otolith morphometry and relative growth. *Neotropical Ichthyology*, 17, e180101.
https://doi.org/10.1590/1982-0224-20180101

Mahé, K., Gourtay, C., Defruit, G.B., Chantre, C., de Pontual, H., Amara, R., Claireaux, G., Audet, C., Zambonino-Infante, J.L. & Ernande, B. (2019) Do environmental conditions (temperature and food composition) affect otolith shape during fish early-juvenile phase? An experimental approach applied to European Seabass (*Dicentrarchus labrax*). *Journal of Experimental Marine Biology and Ecology*, 521, 151239.
https://doi.org/10.1016/j.jembe.2019.151239

Marceniuk, A.P. & Menezes, N.A. (2007) Systematics of the family Ariidae (Ostariophysi, Siluriformes), with a redefinition of the Genera. *Zootaxa*, 1416 (1), 1–126.
https://doi.org/10.11646/zootaxa.1416.1.1

Marceniuk, A.P., Menezes, N.A. & Britto, M.R. (2012) Phylogenetic analysis of the family Ariidae (Ostariophysi: Siluriformes), with a hypothesis on the monophyly and relationships of the genera. *Zoological Journal of the Linnean Society*, 165, 534–669.
https://doi.org/10.1111/j.1096-3642.2012.00822.x

Marceniuk, A.P., Acero, A.P., Cooke, R.G. & Betancur-R, R. (2017) Taxonomic revision of the New World genus *Ariopsis* Gill (Siluriformes: Ariidae), with description of two new species. *Zootaxa*, 4290 (1), 1–42.
https://doi.org/10.11646/zootaxa.4290.1.1

Marceniuk, A.P., Oliveira, C. & Ferraris Jr, C.J. (2024) A new classification of the family Ariidae (Osteichthyes: Ostariophysi: Siluriformes) based on combined analyses of morphological and molecular data. *Zoological Journal of the Linnean Society*, 200, 426–476.
https://doi.org/10.1093/zoolinnean/zlad078

Nolf, D. (1985) Otolithi piscium. *In*: Schultze, H. (Ed.), *Handbook of paleoichthyology*. Gustav Fischer Verlag, Stuttgart, pp. 1–146.

Nolf, D. (2013) *The diversity of fish otoliths, past and present*. Royal Belgian Institute of Natural Sciences.

Ohe, F. (2000) Otoliths of three species belonging to family Ariidae from East China Sea. *Kaseki no Tomo*, 47, 35–42.

Ohe, F. (2006) Skulls and otoliths of eleven sea catfishes (Family Ariidae) from Malaysia and one species related to them from the East China Sea. *Natural Environmental Science Research*, 19, 11–28.

Ponton, D. (2006) Is geometric morphometrics efficient for comparing otolith shape of different fish species? *Journal of Morphology*, 267 (6), 750–757.
https://doi.org/10.1002/jmor.10439

Popper, A.N., Ramcharitar, J. & Campana, S.E. (2005) Why otoliths? Insights from inner ear physiology and fisheries biology. *Marine and freshwater Research*, 56 (5), 497–504.
https://doi.org/10.1071/MF04267

Pusey, B.J., Jardine, T.D., Bunn, S.E. & Douglas, M.M. (2020) Sea catfishes (Ariidae) feeding on freshwater floodplains of northern Australia. *Marine and Freshwater Research*, 71 (12), 1628–1639.
https://doi.org/10.1071/MF20012

Santificetur, C., Giaretta, M.B., Conversani, V.R.M., Brenha-Nunes, M.R., Siliprandi, C.C. & Rossi-Wongtschowski, C.L.D.B. (2017) Atlas of marine bony fish otoliths of Southeastern-Southern Brazil Part VIII: Siluriformes (Ariidae) and Pleuronectiformes (Achiridae, Paralichthyidae, Cynoglossidae). *Brazilian Journal of Oceanography*, 65 (3), 448–494.
https://doi.org/10.1590/s1679-87592017143106503

Santos, L. & Vaz-dos-Santos, A.M. (2023) Insights of otoliths morphology to reveal patterns of teleostean fishes in the Southern Atlantic. *Fishes*, 8 (1), 21.
https://doi.org/10.3390/fishes8010021

Simier, M., Osse, O.J.F., Sadio, O. & Ecoutin, J.M. (2021) Biology and ecology of sea catfish (Ariidae) of estuarine, lagoon and coastal ecosystems in West Africa. *Journal of Fish Biology*, 99 (2), 629–643.
https://doi.org/10.1111/jfb.14751

Souza, A.T., Soukalová, K., Děd, V., Šmejkal, M., Blabolil, P., Říha, M., Jůza, T., Vašek, M., Čech, M., Peterka, J., Vejřík, L., Vejříková, I., Tušer, M., Muška, M., Holubová, M., Boukal, D.S. & Kubečka, J. (2020) Ontogenetic and interpopulation differences in otolith shape of the European perch (Perca fluviatilis). *Fisheries Research*, 230, 105673.
https://doi.org/10.1016/j.fishres.2020.105673

Tuset, V.M., Farré, M., Otero-Ferrer, J.L., Vilar, A., Morales-Nin, B. & Lombarte, A. (2016) Testing otolith morphology for

measuring marine fish biodiversity. *Marine and Freshwater Research*, 67 (7), 1037–1048. https://doi.org/10.1071/MF15052

Vignon, M. (2012) Ontogenetic trajectories of otolith shape during shift in habitat use: Interaction between otolith growth and environment. *Journal of Experimental Marine Biology and Ecology*, 420, 26–32. https://doi.org/10.1016/j.jembe.2012.03.021

Weisler, M.I. (1993) The importance of fish otoliths in Pacific Island archaeofaunal analysis. *New Zealand Journal of Archaeology*, 15, 131–159.

SUPPLEMENTARY MATERIALS. The following supporting information can be downloaded at the DOI landing page of this paper.

Supplementary data 1. Checklist of Southeast Asian modern Ariidae taxa. Information modified from Kailola (1999), Marceniuk *et al.* (2024), and the fishbase website (Froese & Pauly, 2024). **Highlighted in grey**: studied taxa, **Labelled with asterisk (*)**: taxa that can be found in South China Sea.

Supplementary data 2. Photos of Ariidae with elongated otoliths. **1**: *Arius maculatus*; **2**: *Arius oetik*; **3**: *Arius venosus*; **4**: *Batrachocephalus mino*; **5**: *Cryptarius truncatus*; **6**: *Kyataphisa nenga*, **a**: Side view of whole body of the fish, **b**: Dorsal view of head, **c**: Upper tooth patches, **Scale bar**: 5cm.

Supplementary data 3. Photos of Ariidae with elongated and rounded otoliths. Elongated: **1**: *Osteogeneiosus militaris*; Rounded: **2**: *Hexanematichthys sagor*; **3**: *Netuma bilineata*; **4**: *Netuma thalassina*; **5**: *Plicofollis argyropleuron*; **6**: *Plicofollis nella*, **a**: Side view of whole body of the fish, **b**: Dorsal view of head, **c**: Upper tooth patches, **Scale bar**: 5cm.

Supplementary data 4. Dorsal view of the studied ariid taxa neurocranium. **1a**: *Arius maculatus*; **1b**: *Arius oetik*; **1c**: *Arius venosus*; **1d**: *Batrachocephalus mino*; **2a**: *Cryptarius truncatus*; **2b**: *Kyataphisa nenga*, **2c**: *Osteogeneiosus militaris*; **2d**: *Hexanematichthys sagor*; **3a**: *Netuma bilineata*; **3b**: *Netuma thalassina*; **3c**: *Plicofollis argyropleuron*; **3d**: *Plicofollis nella*, **Scale bar**: 1cm.

Supplementary data 5. Left lapillus otoliths of the *Arius* and *Batrachocephalus* genera. **1a–3b**: *Arius maculatus*; **3c–4d**: *Arius oetik*; **4e–10b**: *Arius venosus*; **10c**: *Batrachocephalus mino*, **Scale bar**: 1mm.

Supplementary data 6. Left lapillus otoliths of the *Cryptarius*, *Kyataphisa*, and *Osteogeneiosus* genera. **1a–5b**: *Cryptarius truncatus*; **5c–6c**: *Kyataphisa nenga*, **6d–9b**: *Osteogeneiosus militaris*, **Scale bar**: 1mm.

Supplementary data 7. Left lapillus otoliths of the *Hexanematichthys* and *Netuma* genera. **1a–3b**: *Hexanematichthys sagor*; **3c–7b**: *Netuma bilineata*; **7c–9f**: *Netuma thalassina*, **Scale bar**: 1mm.

Supplementary data 8. Left lapillus otoliths of the *Plicofollis* genera. **1a–6d**: *Plicofollis argyropleuron*; **6e–11b**: *Plicofollis nella*, **Scale bar**: 1mm.

Supplementary table 1. Fish and otolith measurements, along with calculations for each parameter.

Supplementary table 2. Correlation coefficient value for each taxa in each parameter.

Supplementary table 3. Pairwise statistical analysis for parameters RE (rectangularity) and R3 (mesial-distal width) between the elongated and rounded group.

Supplementary table 4. Pairwise statistical analysis for parameter AP4 (central offset) between *N. bilineata* and *N. thalassina*.

Supplementary table 5. Multi-taxa statistical analysis for each selected parameters for each group.

Supplementary table 6. Sample appearance guide.